Original Article *Iran J Ped Hematol Oncol. 2023, Vol 13, No 2, 99-118*

Synergistic Anti-Cancer Effects of Second-Generation Proteasome Inhibitor Carfilzomib with Doxorubicin and Dexamethasone Via p53-Mediated Apoptosis in Pre-B Acute Lymphoblastic Leukemia Cells

Ali Amini PhD[1], Mohammad Faranoush MD[2], Mostafa Paridar MD-PhD[3], Ahmad Kazemi PhD[1], Mohammad Reza Rezvani PhD[1], Majid Safa PhD[1, 4*]

1. Department of Hematology and Blood Banking, Faculty of Allied Medicine, Iran University of Medical Sciences, Tehran, Iran
2. Pediatric Growth and Development Research Center, Institute of Endocrinology and Metabolism, Iran University of Medical Sciences, Tehran, Iran
3. Ministry of Health and Medical Education, Deputy of Management and Resources Development, Tehran, Iran
4. Cellular and Molecular Research Center, Iran University of Medical Sciences, Tehran, Iran
*Corresponding author: Dr. Majid Safa, Department of Hematology and Blood Banking Faculty of Allied Medicine Iran University of Medical Sciences, Hemmat Highway, Tehran, Iran. Postcode: 1449614535. Tel: (+98 21) 8670 4667. Fax: (+98 21) 8862 2578. Email: safa.m@iums.ac.ir. ORCID ID: 0000-0003-0070-6620

Received: 09 April 2021 **Accepted:** 10 January 2023

Abstract

Background: The ubiquitin-proteasome system (UPS) plays a crucial role in regulating the levels and functions of a large number of proteins in the cell, which are important for cancer cell growth and survival. The proteasome is highly activated in B-cell precursor acute lymphoblastic leukemia (BCP-ALL), which is the most common malignancy in children. The attempt to inhibit proteasome as a therapeutic strategy has been successful for some malignancies.

Materials and Methods: In this experimental study, human BCP-ALL cell lines NALM-6 and SUP-B15 were treated with carfilzomib with and without the chemotherapeutic agents. The XTT assay evaluated the viability of the cells. Cell cycle analysis and apoptosis assay were assessed by flow cytometry. RQ-PCR and western blotting evaluated the expression of pro-/anti-apoptotic signals. A drug combination study for synergistic or additive effects of carfilzomib with doxorubicin or dexamethasone was performed.

Results: We observed that carfilzomib alone induced G2/M cell cycle arrest and caspase-dependent apoptosis in the human BCP-ALL cells (NALM-6 and SUP-B15). Gene and protein expression analysis indicated the upregulation of pro-apoptotic as well as downregulation of the cell survival and proliferative signals (P-value<0.05). The synergy of carfilzomib with doxorubicin or dexamethasone was revealed in BCP-ALL cells.

Conclusion: Our results indicated that proteasome inhibition induces p53-mediated apoptosis in BCP-ALL cells. Since carfilzomib has a synergistic effect with anti-leukemic agents doxorubicin and dexamethasone in BCP-ALL cells, this combined-modality approach might be befitting for patients who do not respond well to conventional chemotherapy.

Keywords: Acute lymphoblastic leukemia, Carfilzomib, Dexamethasone, Doxorubicin, Proteasome

[DOI: 10.18502/ijpho.v13i2.12339]

Introduction

Acute lymphoblastic leukemia (ALL) is a malignancy of lymphoid precursor cells within the bone marrow. B-cell precursor ALL (BCP-ALL) is the most common cancer in children, accounting for approximately 30% of all pediatric malignancies and 80% of childhood leukemia. Its incidence has a two-peak distribution, with the first peak occurring in childhood (80%) and the second peak nearly at about 50 years of age (1). The pathogenesis of the disease often involves genetic abnormalities that alter the genes controlling cell proliferation and survival of the lymphoblasts. Currently, the first-line treatment in these patients is chemotherapy, which includes a combination of drugs such as vincristine, corticosteroids, asparaginase, and anthracyclines. Despite long-term survival and high rates of treatment in most

children with BCP-ALL, relapse and resistance to treatment are the leading cause of death (2). Therefore, augmenting the therapeutic armamentarium against BCP-ALL is crucial.

Cell fate is controlled by a balance between cell cycle regulators (cyclin-dependent kinases, p21, p27, c-myc, hTERT, p25, etc.) pro-apoptotic (p53, Bim, Bax, Noxa, Bid, Bak, Puma, etc.) and anti-apoptotic (Bcl-2, Bcl-xl, c-IAP1/2, XIAP, survivin, Mcl-1, etc.) signals, most of which are regulated by the ubiquitin-26S proteasome system (UPS). The UPS is a multi-catalytic proteinase complex that breaks down a wide range of proteins within normal and transformed cells and therefore plays a crucial role in maintaining cellular homeostasis. Consequently, UPS can affect pivotal cellular functions such as cell cycle, DNA repair, apoptosis, cell growth, and survival (3). The 26S proteasome contains a hollow central 20S proteolytic structure and two 19S helices regulating the entry of target proteins at its two ends. The 20S core has three enzymatically active sites: caspase-like (C-L), chymotrypsin-like (CT-L), and trypsin-like (T-L) (4). High proteasome activity has been demonstrated in several malignancies, particularly in hematological neoplasms (5). The application of proteasome inhibitors (PIs) as a front-line treatment in multiple myeloma patients represents UPS as a valid target in the treatment of malignant diseases (3). Since selective inhibition of CT-L has a slight impact on overall cellular protein turnover, PIs that inhibit only the CT-L subunit is considered optimal. Among the PIs, bortezomib, carfilzomib, and ixazomib have been approved by the FDA, mostly for patients with multiple myeloma progressing after initial treatment (6, 7).

Although bortezomib, as the first FDA-approved PI, has proven to be successful in treating multiple myeloma patients, the progression of neuropathy and recurrence after treatment are the most important complications. Second-generation proteasome inhibitors such as carfilzomib were developed due to the adverse effects of bortezomib or the development of resistance in some patients. Moreover, carfilzomib was tolerable in combination with VXLD (vincristine, dexamethasone, PEG-asparaginase, daunorubicin) chemotherapy in phase I of a clinical study in T-ALL patients (8). Approximately half of all cancers bear mutated p53, but in the other half of tumors, wild-type p53 is inactivated through various mechanisms (9). Towards this end, restoring p53 activity in tumor cells has been a long-sought-after goal. Wild-type p53 is a master regulator of apoptosis and the cell cycle is tightly kept at low levels via degradation by the proteasome (9, 10). Therefore, inhibition of the proteasome in BCP-ALL cells, which most often express wild-type p53, can reinstate p53 function and might be considered as an adjunctive therapy together with key drugs for the treatment of BCP-ALL such as anthracyclines. Since PIs can target critical molecular pathways that are involved in the survival and proliferation of BCP-ALL cells, we intended to investigate the effects of carfilzomib in the BCP-ALL cells. In addition, synergistic experiments were carried out to evaluate the potential effects of carfilzomib on the anti-cancer effects of doxorubicin and dexamethasone.

Materials and Methods

Chemicals and reagents

Carfilzomib was from Selleck Chemicals (Houston, Texas, USA); Dexamethasone (D4902), doxorubicin and propidium iodide (PI) were from Sigma-Aldrich (St Louis, Missouri, USA). For immunoblotting, primary antibodies including caspase-3 (Cat. #: 9665), caspase-9 (9508), PARP (9542), p21 (2947), p53 (2527), p27 (2552), c-Myc (5605), c-IAP1(4952), XIAP (2045), survivin (2808), Bax (2772), Bcl-2 (15071), Bcl-xl (2764), Mcl-1 (94296), and β-actin (8H10D10) were provided from Cell Signaling Technology (Danvers,

[DOI: 10.18502/ijpho.v13i2.12339]

Massachusetts, USA). HRP-conjugated secondary antibodies were purchased from Santa Cruz Biotechnology (Santa Cruz, California, USA).

Cell culture

The human BCP-ALL cell lines NALM-6 (obtained from Pasteur Institute, Tehran, Iran) and SUP-B15 **(**provided by Dr. Parviz Kokhaei, Department of Immunology, Semnan University of Medical Sciences) were cultured in RPMI-1640 medium enriched with L-glutamine (2 mM), heat-inactivated 10% FBS (20% for SUP-B15), penicillin (100 units/ml), and streptomycin (100 µg/ml) in a humidified 37 ºC incubator with 5% CO_2 within up to 10 passages from thawing.

Cell viability assay

Cell viability was measured by the colorimetric XTT-based assay (Roche, Penzberg, Germany). In brief, NALM-6 and SUP-B15 cells were seeded into 96-well-cultured plates at ~1×10^4 cells/well. The cells were treated with various concentrations of carfilzomib alone (5, 10, and 20 nM for NALM-6 and 2, 4, and 8 nM for SUP-B15) and followed by treatment with doxorubicin (100 and 200 nM) or dexamethasone (200 and 400 nM) for 24 and 48 h (whereas 72 h for combination with dexamethasone in NALM-6 cells). Next, 50 µl of XTT reagent was added to cells and incubated for 18 h at 37 ºC. The absorbance of each well at 450 nm was read using an ELISA reader (Bio-Rad; Hercules, California, USA).

Drug combination study

Combination index (CI) values were estimated from dose-effect data. CompuSyn software (ComboSyn, Inc., Paramus, NJ) was used for standard isobologram analysis. Combinations were then scored according to the following criteria: The CI values of <1, =1, and, >1 represent the synergistic, additive, and antagonistic activity of drugs, respectively

Cell cycle analysis

To measure DNA content, a total of 2×10^5 cells/ml were seeded in 12-well-cultured plates and incubated with different concentrations of carfilzomib (5, 10, and 20 nM for NALM-6 and 2, 4, and 8 nM for SUP-B15) for 24 h. Cells were collected after incubation time, washed two times with PBS, and subsequently fixed in ice-cold 70% ethanol overnight at -20 C. Then, the cells were washed with cold PBS and resuspended in PBS containing 0.1% sodium citrate, 0.5 µg/ml RNase (Thermo Scientific, Waltham, Massachusetts, USA), and propidium iodide (50 µg/ml). The cells were protected from light at room temperature for 30 minutes and then analyzed using a FACSCalibur flow cytometer (BD Biosciences, San Jose, California, USA).

Flow cytometry analysis of apoptosis

The cells were cultured in 12-well plates at a density of 2×10^5 cells/ml and incubated with different concentrations of carfilzomib alone for 24 h and 48 h. In addition, both cell lines were treated with different doses of carfilzomib in the presence of doxorubicin (100 and 200 nM for NALM-6, 20 and 40 nM for SUP-B-15) for 24 h. Likewise, dexamethasone treatment (200 and 400 nM for NALM-6, 20 and 40 nM for SUP-B-15) with carfilzomib was done for 24 h on SUP-B15 and 72 h for NALM-6 cells. After incubation, harvested cells were washed with cold PBS (Phosphate-buffered saline), and stained using Annexin V-FITC Apoptosis Detection Kit II (BD Biosciences) according to instructions of the manufacturer. Annexin V positive and PI negative cells show early apoptotic cells; while both Annexin V and PI positive cells represent a late apoptosis phase.

RNA extraction, cDNA synthesis, and RQ-PCR

Total RNA was extracted by TriPure isolation reagent (Roche Applied Science)

[DOI: 10.18502/ijpho.v13i2.12339]

from treated and untreated cells. Next, according to the RevertAid First Strand cDNA Synthesis kit protocol (Thermo Scientific, Waltham, Massachusetts, USA), 1 µg of RNA was reverse transcripted into cDNA using a master mix containing 4 µl 5X Reaction Buffer, 1 µl RNase inhibitor (20 U/ml), 1 µl M-MuLV reverse transcriptase (200 U/ml), 2 µl dNTP Mix (10 mM), 1 µl random hexamers and Nuclease-free water up to final volume 20 µl. Quantitative real-time PCR was performed in a total volume of 15 µl using 2 µl of specific gene primers, 1.5 µl of the cDNA product, and 7.5 µl of RealQ Plus 2X Master Mix Green without ROX (Ampliqon, Odense, Denmark) according to the manufacturer's instructions in a Light Cycler 96 Real-time PCR system (Roche Diagnostics, Lewes, UK). PCR amplification was performed using the following conditions: 95 ºC for 15 min followed by 35 cycles of 95 ºC for 15 s, and annealing and elongation step at 60 ºC for 60 s. Each sample was analyzed in triplicate, the specificity of the products was verified using melting curve analysis, and the comparative *Ct* ($2^{-\Delta\Delta Ct}$) method for calculation of fold-change in the gene expression was used. Primer sequences of Bax, Bim, Noxa, Bcl-2, Mcl-1, survivin, c-Myc, hTERT, p27 and β-Actin used for real-time PCR analysis are listed in Table I.

Western blot analysis

A total of 5×10^6 cells/aliquots were centrifuged after the treatments and cellular pellets were washed twice with cold PBS. The cellular proteins were extracted with 0.2 ml of RIPA lysis buffer (150 mM NaCl, 10 mM Tris-HCl, pH 7.4, 5 mM EDTA, 0.1% SDS, 1% Triton X-100, 50 mM NaF, 0.5% sodium deoxycholate, and 1 mM NaVO4) containing protease and phosphatase inhibitor cocktails (Sigma-Aldrich, St. Louis, Missouri, USA) on ice for 30 min. After centrifugation at 13000 rpm at 4°C for 20, the supernatant was gathered. Bradford assay was used for the determination of protein concentrations. Equal amounts of total cellular protein (70 µg in a total volume of 24 µl) were loaded and resolved on 10% SDS-PAGE, according to the method of Laemmli. To determine molecular weight, a multicolor protein ladder (size ranges of 10-190 kDa and 40-300 kDa) was employed as a standard. The gels were then electroblotted onto nitrocellulose membranes (Hybond-ECL; Amersham Corp., Little Chalfont, UK) for 1 h under 60 V. Afterward, blocking of membranes was performed for 1 h at room temperature with 5% skim milk diluted in TBS with 0.1% Tween-20 (TBS-T). Then, the membranes were hybridized with specific primary antibodies (1:1000 dilution) at 4°C overnight. After incubation, membranes were washed 5 times in TBS-T and incubated with HRP-conjugated secondary antibodies (1:5000 dilution). Protein expression was detected by, chemiluminescence reagent (Amersham ECL Advance Kit; GE Healthcare, Little Chalfont, UK) according to the manufacturer's recommendation using ChemiDoc instrument (Vilber Lourmat SAS, France).

Statistical analysis

The experiments were carried out in triplicate, and data were presented as the mean ± standard deviation. Statistical differences between the two groups were tested with Paired Student's *t*-test. A *P*-value was considered significant if less than 0.05. Statistical analysis was applied using Prism 6.01 software (GraphPad, La Jolla, California, USA).

Ethical consideration

This study was approved by the Ethics Committee of Iran University of Medical Sciences (IR.IUMS.REC1395.9221534201).

[DOI: 10.18502/ijpho.v13i2.12339]

Results

Proteasome inhibition induced prominent dose- and time-dependent cytotoxicity in BCP-ALL cell lines

The viability of BCP-ALL cells upon treatment with carfilzomib was determined by XTT assay. Both NALM-6 and SUP-B15 cells were incubated with designated concentrations of carfilzomib for 24 and 48 h. As shown in Fig. 1a, a significant dose and time-dependent decrease in the survival of NALM-6 and SUP-B15 cells treated with carfilzomib was observed. The highest cytotoxicity was observed at 48 h at 20 (IC_{50}: 7.5 nM) and 8 nM of carfilzomib (IC_{50}: 3 nM) for NALM-6 and SUP-B15 cells, respectively (*P*-value= 0.0002).

Carfilzomib synergistically intensified the cytotoxic effect of doxorubicin and dexamethasone on BCP-ALL cells

Given the potential role of carfilzomib to induce cytotoxicity in BCP-ALL cells, it was tempting to evaluate whether carfilzomib potentiates the cytotoxic effects of doxorubicin and dexamethasone. To do so, we examined carfilzomib's effects either as a single agent or in combination with doxorubicin or dexamethasone on the viability of BCP-ALL cells. Based on the synergistic analysis, we observed that carfilzomib co-treatment with doxorubicin or dexamethasone was highly effective in growth inhibition and enhancing the cytotoxic effect relative to either drug alone (Fig. 1b and c). Moreover, to determine whether the interaction between any of these agents was synergistic or additive, the CI value was calculated (Table II). Synergistic experiments delineated that pharmaceutical targeting of the proteasome with carfilzomib could potentiate the anti-cancer effect of both doxorubicin and dexamethasone (Fig. 1b and c).

Carfilzomib stimulated G2/M cell cycle arrest in BCP-ALL cells

To better understand whether the inhibitory effect of proteasome inhibition on the proliferation of BCP-ALL cells is related to cell cycle alteration or not, we sought to evaluate the effect of carfilzomib on the cell cycle of the BCP-ALL cell lines using flow cytometric analysis. As depicted in Fig. 2, following 24 h treatment of NALM-6 and SUP-B15 cells with different doses of carfilzomib, a reduction in the S phase and a significant accumulation in the G2/M phase was observed, especially at higher doses of carfilzomib.

Proteasome inhibition accentuated doxorubicin/dexamethasone-induced caspase-mediated apoptosis in BCP-ALL cells

To investigate the effect of proteasome inhibition on cell apoptosis, BCP-ALL cells were incubated with different concentrations of carfilzomib alone and in combination with doxorubicin or dexamethasone. Then, cells were harvested and stained with Annexin V-PI, followed by flow cytometry analysis. As demonstrated in Fig. 3a and b, the percentage of early and late apoptotic cells after treatment with the escalating doses of carfilzomib exhibited a significant increase compared to the untreated cells. Furthermore, we observed that carfilzomib co-treatment with anti-leukemic agents doxorubicin or dexamethasone increased the number of Annexin-V+/PI+ cells in both NALM-6 and SUP-B15 cells in comparison to either agent alone (Fig. 3 c and d). Activation of caspase-3/9 and poly (ADP-ribose) polymerase (PARP) cleavage was examined by western blotting to confirm the molecular basis of the apoptosis process. As presented in Fig. 4a to 4c, carfilzomib induced prominent cleavage of caspase-3, caspase-9, and PARP proteins relative to the control cells. Interestingly, the combination of carfilzomib with doxorubicin or

[DOI: 10.18502/ijpho.v13i2.12339]

dexamethasone greatly induced PARP cleavage and caspase activation compared with either agent alone. These results suggest that inhibition of proteasome by carfilzomib substantially potentiates the apoptotic activity of chemotherapeutic agents doxorubicin and dexamethasone in BCP-ALL cells.

Carfilzomib triggered apoptosis through the regulation of pro- and anti-apoptotic molecules

To comprehend the probable underlying mechanisms of the carfilzomib-induced apoptosis in BCP-ALL, NALM-6, and SUP-B15 cells were subjected to treatment with various doses of carfilzomib for 24 h and then analyzed for the expression of Bax, Bim, Noxa, Bcl-2, Mcl-1, survivin, Bcl-xl, XIAP, and c-IAP1 levels by real-time PCR and western blotting. The results showed a significant upregulation in pro-apoptotic genes, including Bax, Bim, and in particular, Noxa. The expression of Bax mRNA and protein was increased in BCP-ALL cells. Carfilzomib significantly reduced the expression of the anti-apoptotic proteins such as Bcl-2, Bcl-xl, survivin, XIAP, and c-IAP1 (Fig. 5a). Intriguingly, the expression of anti-apoptotic gene Mcl-1 was upregulated upon carfilzomib treatment in both mRNA and protein levels. It's worth mentioning that the expression levels of the evaluated genes and proteins were affected at the lower concentration of the inhibitor in SUP-B15 cells relative to NALM-6 cells. We then investigated how apoptotic-related genes were affected by carfilzomib co-treatment with doxorubicin or dexamethasone. To this end, after incubation of the cells with doxorubicin or dexamethasone in the absence or presence of carfilzomib, the aforementioned genes were studied. As shown in Fig. 5b and c, a striking increase in the expression of pro-apoptotic genes, including Bax, Bim, and Noxa, was observed in the combination treatment. Likewise, the expression of Bax protein upregulated in BCP-ALL cells after carfilzomib co-treatment with the chemotherapeutic agents (Fig. 5d). Doxorubicin alone increased Bcl-2 expression; whereas, it decreased significantly in the presence of carfilzomib, indicating that carfilzomib inhibited doxorubicin-induced Bcl-2 gene expression. Unlike the elevated expression levels of Mcl-1, lower expression of anti-apoptotic proteins such as Bcl-xl, survivin, XIAP, and c-IAP1 was exhibited upon exposure of the cells to combination of carfilzomib and the anti-leukemic drugs in comparison to either the chemotherapeutic agents individually (Fig. 5d). Generally, our results showed that carfilzomib alone and particularly in combination with doxorubicin or dexamethasone, provokes apoptosis in BCP-ALL cells, presumably by disrupting the transcriptional equilibrium between the death-repressor and the death-promoter signals.

Proteasome inhibition disrupted the cell cycle regulators in a p53-dependent manner

Consistent with the antiproliferative effect of carfilzomib, the results of DNA content analysis also outlined that the inhibition of proteasome potentially induces cell cycle arrest in BCP-ALL cells. Therefore, to shed light on the mechanisms through which carfilzomib induces its effect on the cell cycle regulating molecules in BCP-ALL cells, NALM-6 and SUP-B15 cells were treated with designated concentrations of carfilzomib for 24 h. Then, protein expression of p53, p21, p27, and c-Myc were investigated by western blotting, and transcriptional expression levels of p27, c-Myc, and hTERT were also evaluated by RQ-PCR. The turnover of p53, as well as several key p53 targets, are regulated by the proteasome (11). As indicated in Fig. 6a, in both cell lines upon treatment with carfilzomib, there was a considerable dose-dependent accumulation of p53, p21, and p27 proteins compared to untreated cells. Likewise, after combination treatment, a greater

[DOI: 10.18502/ijpho.v13i2.12339]

accumulation of p53 along with p21 and p27 versus each agent alone was seen in the cell lines (Fig. 6b and c). Furthermore, we observed a marked upregulation of p27 mRNA that correlated with carfilzomib-induced cell cycle arrest. It is well known that several genes, including the proto-oncogene c-Myc, are negatively regulated by the tumor suppressor p53 (12). Constitutive expression of the c-Myc protein exerts a promoting impact on cell proliferation presumably via positive regulation of the catalytic subunit of human telomerase reverses transcriptase (hTERT) expression (13). Moreover, a growing body of evidence revealed that in a variety of cancer cells, overexpression of p21 is associated with repression of hTERT expression (14). Interestingly, our findings showed that a prominent reduction of c-Myc in both NALM-6 and SUP-B15 cells was accompanied by the downregulation of hTERT, which could be due to the elevated p21 and p53 proteins.

Table I: Sequence of the primers used for RQ-PCR.

Gene	Forward primer (5′– 3′)	Reverse primer (5′– 3′)
β-Actin	GGAAATCGTGCGTGACATTAAG	GAAGGAAGGCTGGAAGAGTG
Bcl-2	ATCGCCCTGTGGATGACTGAG	CAGCCAGGAGAAATCAAACAGAGG
Mcl-1	CCAAGAAAGCTGCATCGAACC	AAACCCATCCCAGCCTCTTTG
Bim	CTGACTCTCGGACTGAGAAACG	CTTGTGGCTCTGTCTGTAGGG
Bax	GTCCTCGGATTCTCTGCTCTC	CAACATCGATTTCTTCCTCATCTTC
Survivin	CCAGATGACGACCCCATAGAG	TTGTTGGTTTCCTTTGCAATTTT
c-Myc	GTCCTCGGATTCTCTGCTCTC	CAACATCGATTTCTTCCTCATCTTC
hTERT	ATGCGACAGTTCGTGGCTCA	ATCCCCTGGCACTGGACGTA
p27	GAATAAGGAAGCGACCTGCAACC	TCTTCTGAGGCCAGGCTTCTTG
Noxa	CCGTGTGTAGTTGGCATCTC	CCCACTCAGCGACAGAGC

Table II: Combination indices for BCP-ALL cell lines treated with indicated doses of carfilzomib in combination with either doxorubicin or dexamethasone.

NALM-6					
Dose	**CFZ 7.5 nM**	**CFZ 10 nM**		**CFZ 4 nM**	**CFZ 8 nM**
DOX 100 nM	0.697	0.612	**DEXA 200 nM**	1.391	0.417
DOX 200 nM	0.697	0.510	**DEXA 400 nM**	0.482	0.378
SUP-B15					
	CFZ 3 nM	**CFZ 6 nM**		**CFZ 3 nM**	**CFZ 6 nM**
DOX 20 nM	1.110	0.667	**DEXA 20 nM**	0.534	0.564
DOX 40 nM	0.746	0.403	**DEXA 40 nM**	0.518	0.397

[DOI: 10.18502/ijpho.v13i2.12339]

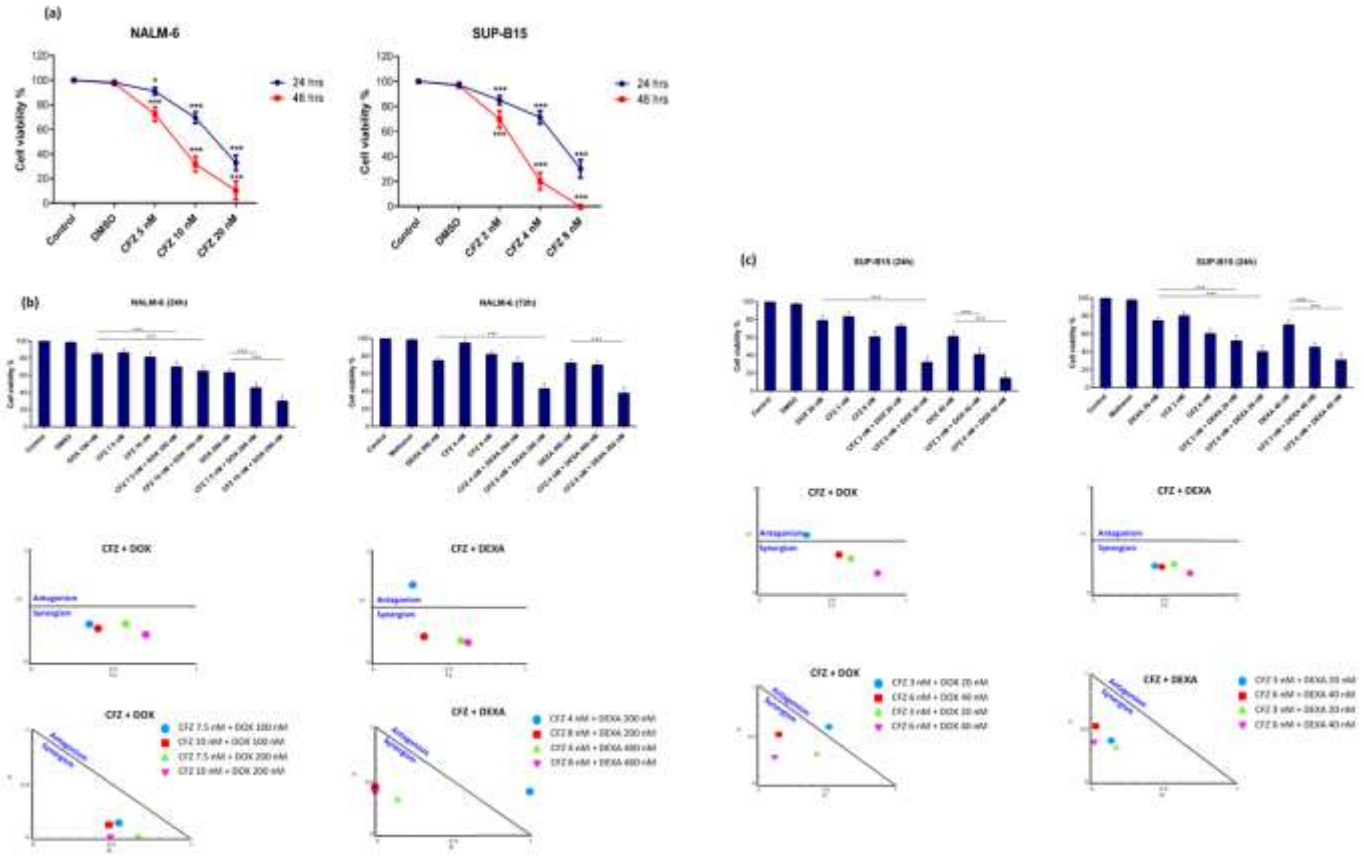

Figure 1. Carfilzomib (CFZ) attenuates cell viability and potentiates doxorubicin/dexamethasone-induced growth inhibition in BCP-ALL cell lines. **(a)** NALM-6 and SUP-B15 cells were treated with increasing concentrations of carfilzomib for 24 and 48 h. Cell growth was measured by the colorimetric XTT-based assay. The viability of BCP-ALL cells treated by carfilzomib was decreased in a time- and dose-dependent manner. The results are presented as the mean ± standard deviations (SD) of at least three independent experiments. *P < 0.05, ***P < 0.001, compared to control cells (Student's t-test, two-tailed). **(b)** NALM-6 and **(c)** SUP-B15 cells were co-treated with various concentrations of carfilzomib and the escalating doses of doxorubicin (DOX) or dexamethasone (DEXA) for indicated time points. Cell viability was evaluated by the XTT assay. The combination index (CI) was calculated according to the classic isobologram equation. Results of synergistic analyses have shown that inhibition of the proteasome could sensitize both BCP-ALL cells to the anti-leukemic activity of doxorubicin or dexamethasone. Each value represented the average of three independent experiments ± SD. *P < 0.05, ***P < 0.001 compare to doxorubicin or dexamethasone alone (Student's t-test, two-tailed)

[DOI: 10.18502/ijpho.v13i2.12339]

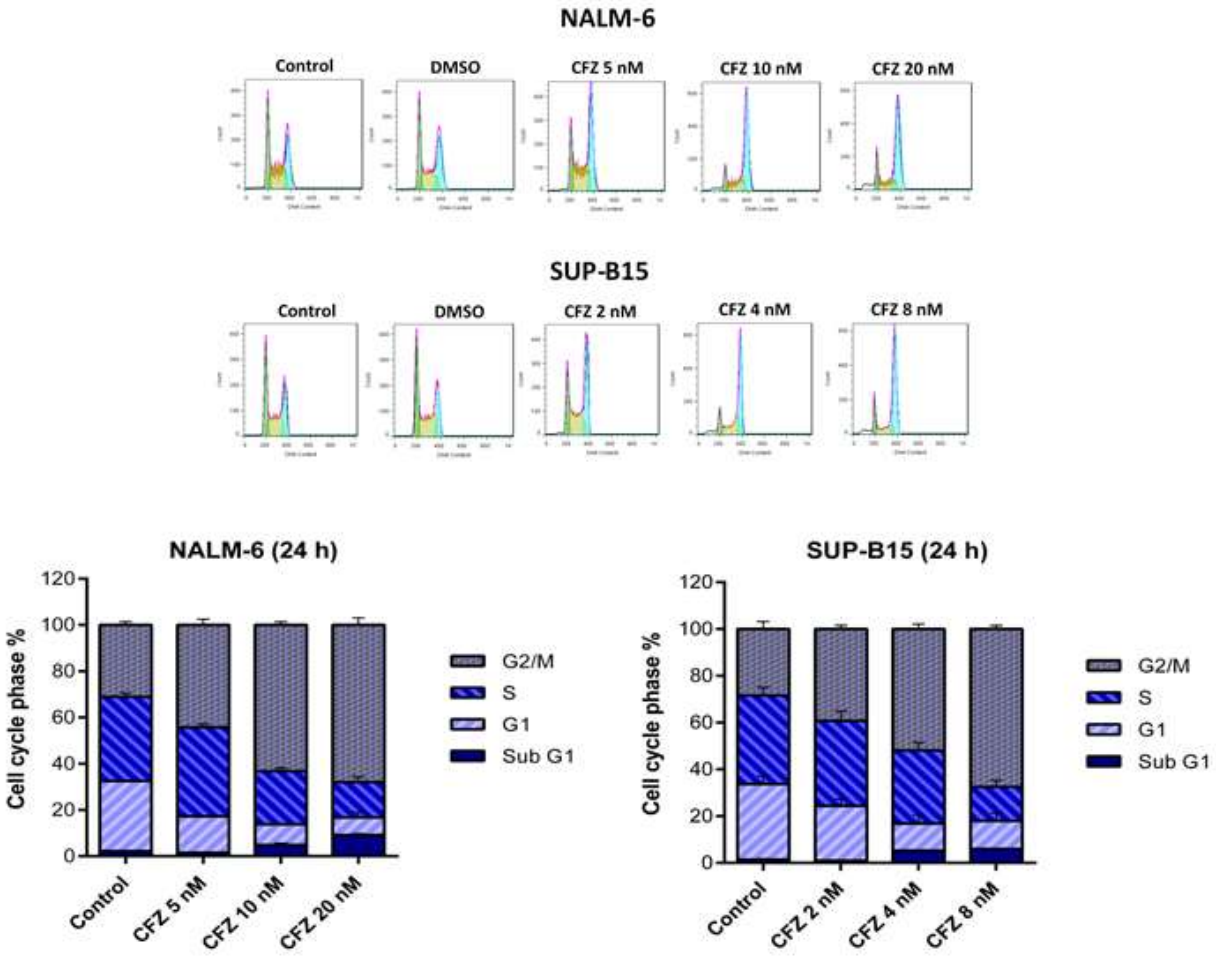

Figure 2. Effects of carfilzomib (CFZ) on cell cycle progression in BCP-ALL cells. NALM-6 and SUP-B15 cells were cultured in complete medium with various doses of carfilzomib for 24 h, and cell cycle distribution was evaluated by flow cytometry. Increased concentrations of carfilzomib resulted in a significant accumulation of the cells in G2/M phase and also a decline in S phase. One representative experiment among three performed experiments is presented. The data are presented as the mean ± SD

[DOI: 10.18502/ijpho.v13i2.12339]

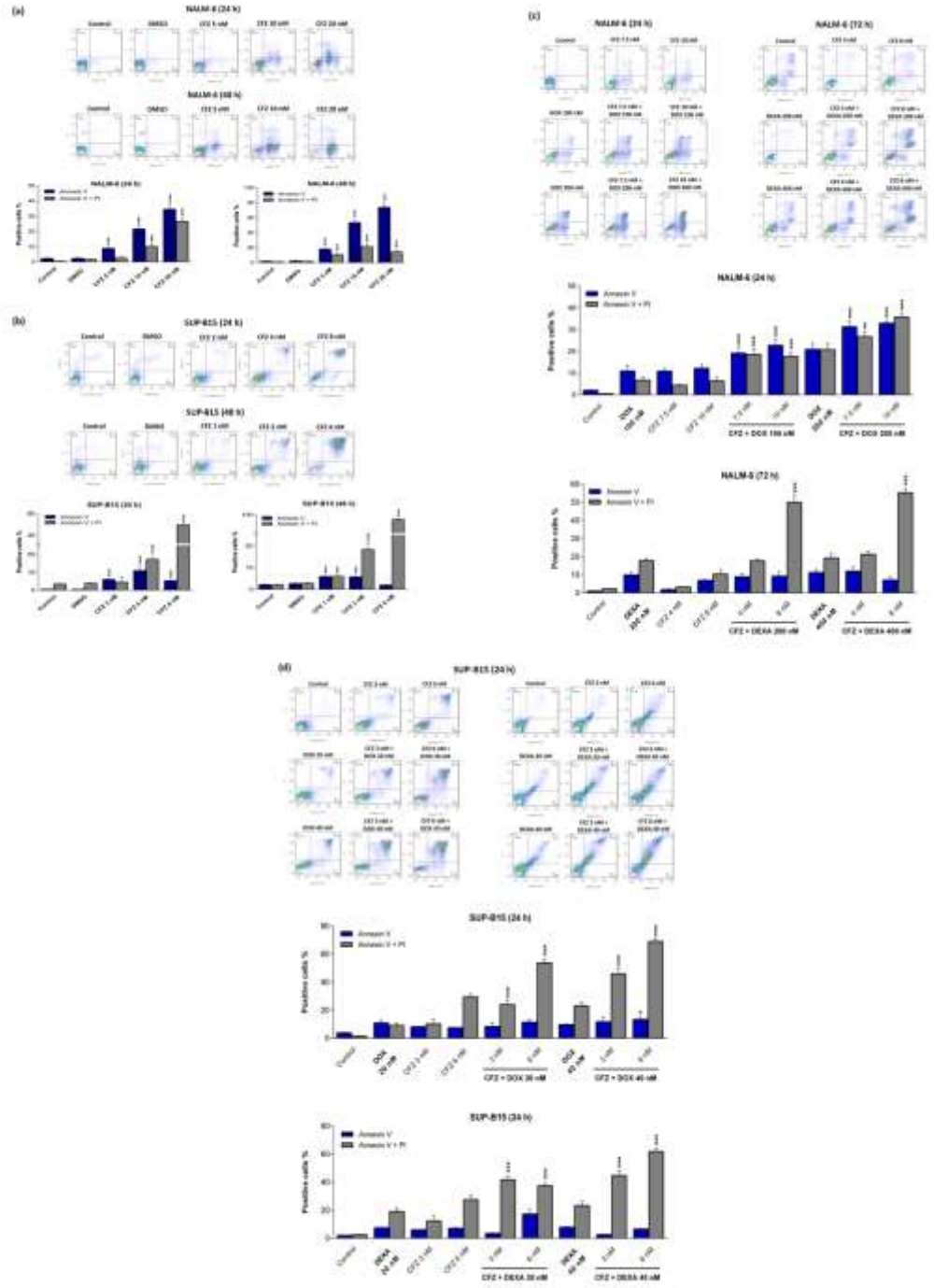

Figure 3. Apoptotic effect of carfilzomib (CFZ) alone and in combination with doxorubicin (DOX) or dexamethasone (DEXA) on BCP-ALL cells. (a) NALM-6 cells were cultured with various concentrations of carfilzomib (5, 10, and 20 nM) for 24 and 48 h. (b) SUP-B15 cells were incubated with different doses of carfilzomib (2, 4, and 8 nM) for 24 and (1, 2, and 4 nM) 48 h. The cells were subjected to Annexin V-PI staining analyzed by flow cytometry. One representative experiment of at least three experiments conducted is shown. *P < 0.05, ***P < 0.001 (Student's t-test, two-tailed), compared to the control cells. The results are presented as the mean ± SD. (c) NALM-6 and (d) SUP-B15 cells were incubated with various doses of carfilzomib followed by designated concentrations of doxorubicin or dexamethasone for 24 h (whereas 72 hours for combination with dexamethasone in NALM-6 cells). Then, the cells were analyzed for Annexin V-PI uptake by flow cytometry. Data are presented as the mean ± SD of at least three independent experiments. *P < 0.05, **P < 0.01, ***P < 0.001 (Student's t-test, two-tailed) compared to doxorubicin or dexamethasone alone

[DOI: 10.18502/ijpho.v13i2.12339]

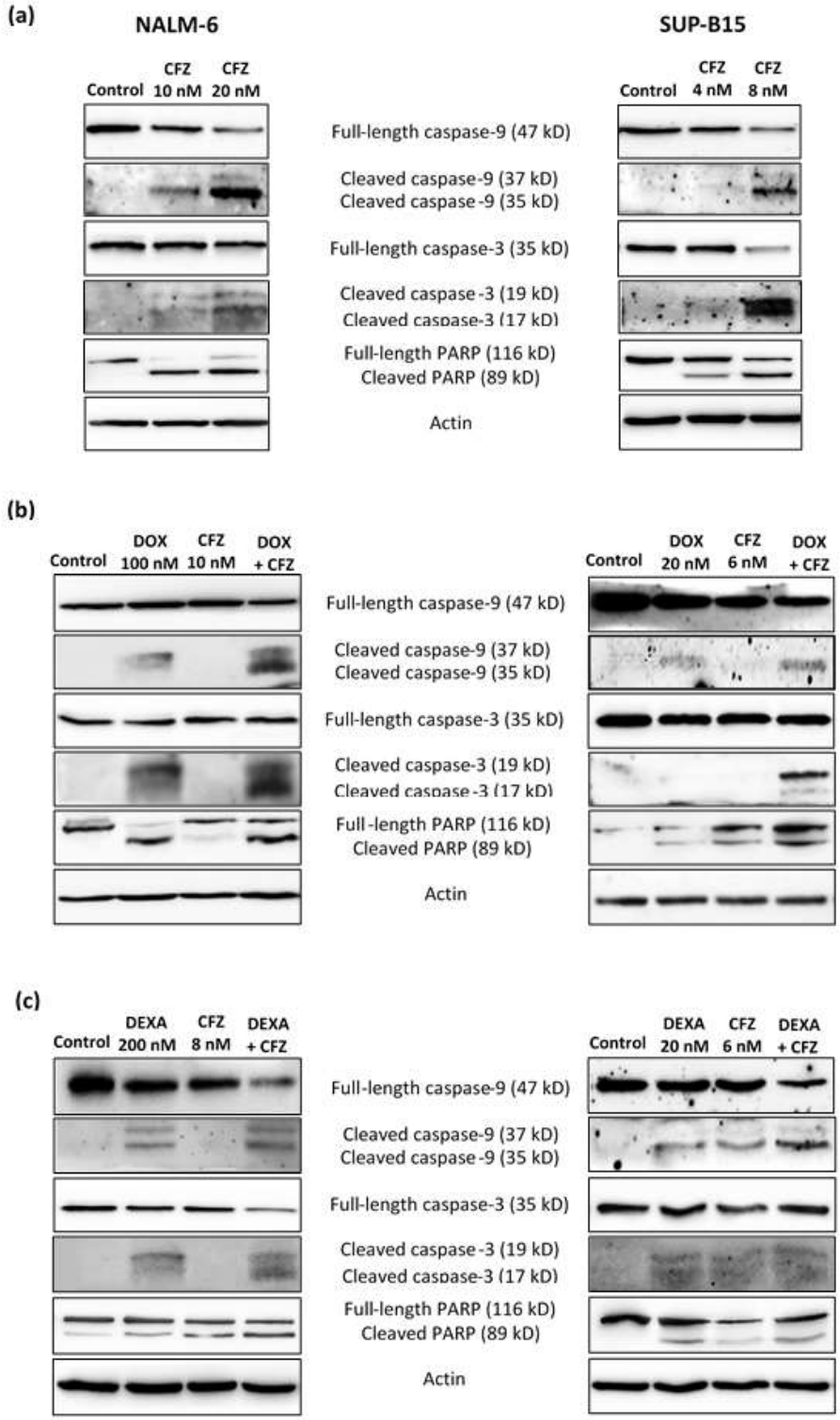

Figure 4. Effect of carfilzomib (CFZ) in the presence or absence of doxorubicin (DOX) and dexamethasone (DEXA) on caspase activation and PARP cleavage. (a) NALM-6 and SUP-B15 cells were treated with various concentrations of carfilzomib alone for 24 h, (b) NALM-6 and SUP-B15 cells were incubated with carfilzomib in combination with doxorubicin for 24 h, (c) NALM-6 and SUP-B15 cells were cultured with carfilzomib in combination with dexamethasone for 72 h and 24 h, respectively. Next, total cell lysates were prepared. Equal amounts of cell lysates (60 µg) were subjected to western blot analysis for cleavage of caspase-9, caspase-3, and PARP. The immunoblots are representative of three independent experiments

[DOI: 10.18502/ijpho.v13i2.12339]

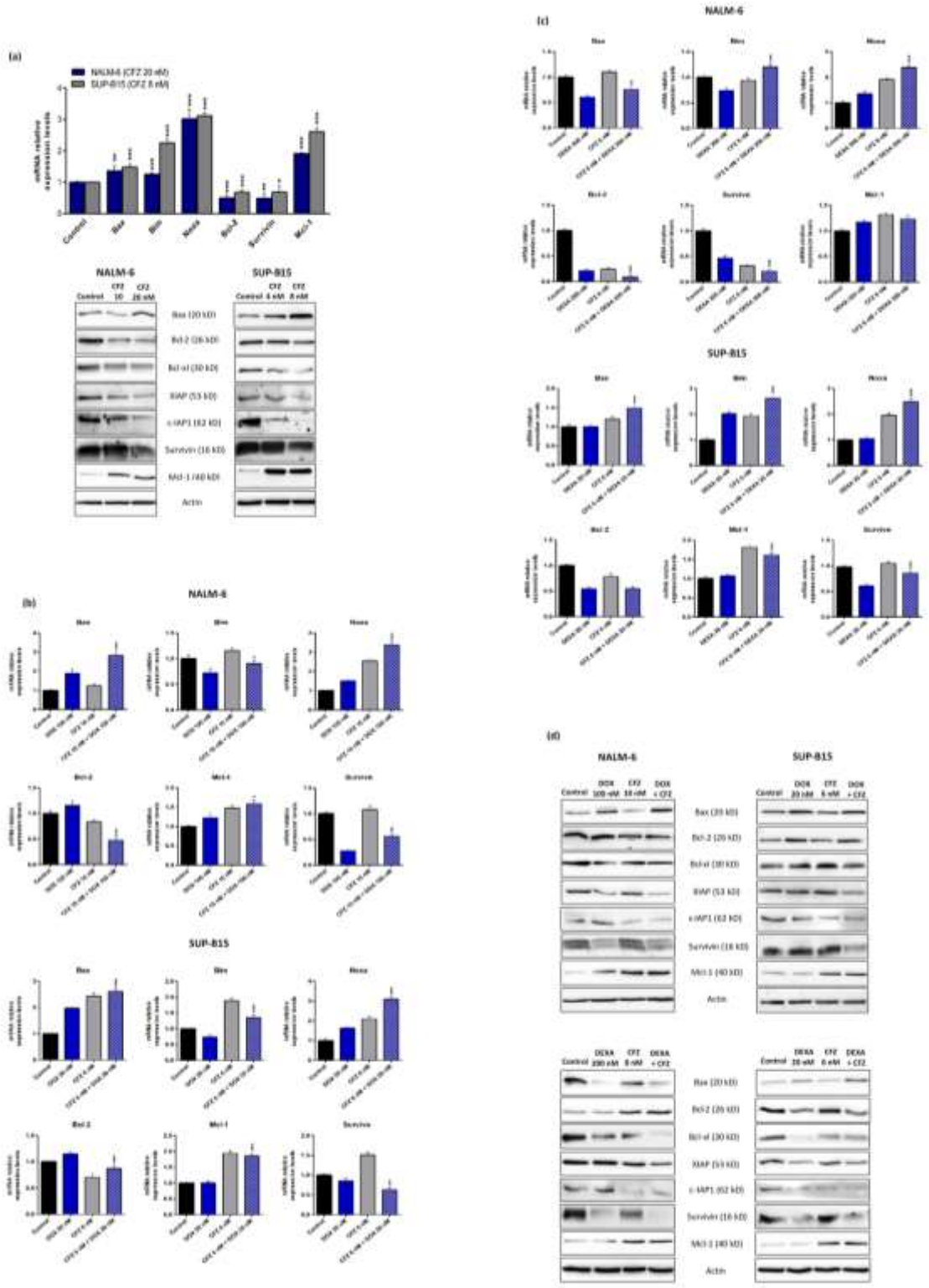

Figure 5. Apoptosis induced by carfilzomib (CFZ) and potentiation of doxorubicin/dexamethasone-induced cell death is mediated via disruption of pro- and anti-apoptotic signals expression balance. (a) NALM-6 and SUP-B15 cells were incubated with carfilzomib (20 and 8 nM respectively) for 24 h, and then the expression of Bax, Bim, Noxa, Bcl-2, Mcl-1, and survivin was measured using quantitative real-time PCR and normalized to the expression of β-actin (n = 3, *P < 0.05, **P < 0.01, ***P < 0.001 (Student's t-test, two-tailed) relative to the control cells. The results are presented as the mean ± SD). Likewise, total cell lysates were prepared, and immunoblotting was performed using specific antibodies against Bax, Bcl-2, Bcl-xl, XIAP, c-IAP, survivin, Mcl-1, and β-actin. One

[DOI: 10.18502/ijpho.v13i2.12339]

representative experiment among three performed experiments is shown. (b) NALM-6 and SUP-B15 cells were treated with carfilzomib in combination with doxorubicin (DOX), and RQ-PCR was performed for gene expression analysis. (c) NALM-6 and SUP-B15 cells were treated with carfilzomib in combination with dexamethasone (DEXA), and expression of the genes was measured by RQ-PCR and normalized to the expression of β-actin (n = 3, *P < 0.05, **P < 0.01, ***P < 0.001 (Student's t-test, two-tailed) compare to doxorubicin/dexamethasone alone. The results are presented as the mean ± SD). (d) Both BCP-ALL cell lines were treated as mentioned above. Then protein levels of the cell survival molecules were detected using western blot. The immunoblots are representative of three independent experiments

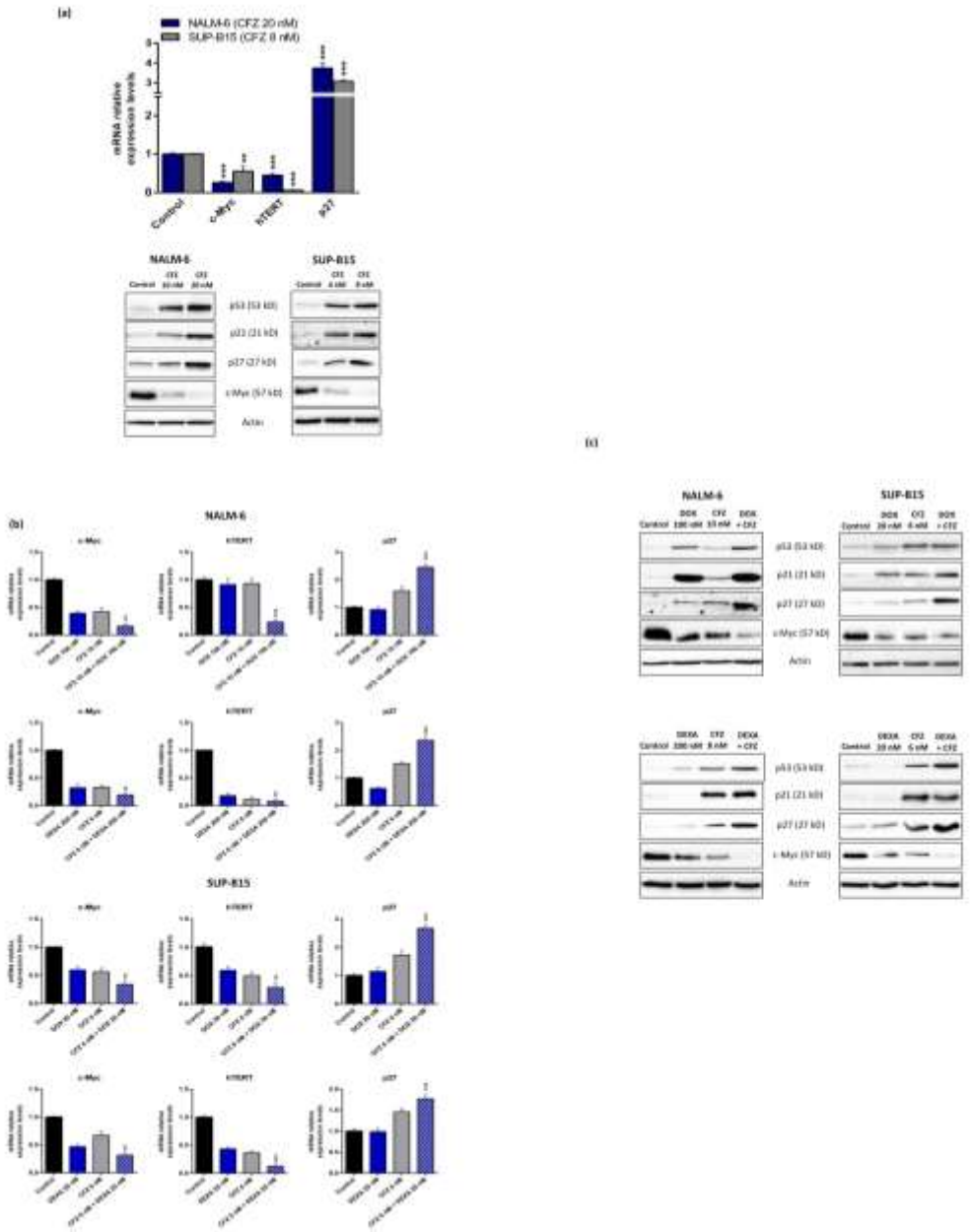

Figure 6. Carfilzomib (CFZ) alone and in combination with doxorubicin/dexamethasone inhibits cell growth by interfering with cell cycle regulatory molecules and induce p53-mediated apoptosis. (a) Downregulation of c-Myc and hTERT, and upregulation of p27 following carfilzomib. After treatment of BCP-ALL cells with different concentrations of carfilzomib for 24 h, total cellulra RNA was extracted, and expression of indicated genes was evaluated by quantitative real-time PCR and normalized to the expression of β-actin (n = 3, **P < 0.01, ***P < 0.001 (Student's t-test, two-tailed)

[DOI: 10.18502/ijpho.v13i2.12339]

relative to untreated cells. The data are presented as the mean ± SD). Furthermore, NALM-6 and SUP-B15 cells were grown in the presence of various doses of carfilzomib for 24 h; cell lysates were prepared, and immunoblot analysis was performed with antibodies specific to p53, p21, p27, and c-Myc. All immunoblots are representative images from at least three independent experiments. In addition, both cell lines were incubated with various doses of carfilzomib followed by designated concentrations of doxorubicin (DOX) and dexamethasone (DEXA); (b) Total cellular RNA was extracted, and expression of aforementioned genes was measured by RQ-PCR and normalized to the expression of β-actin (n = 3, **P < 0.01, ***P < 0.001 (Student's t-test, two-tailed) relative to doxorubicin or dexamethasone. The data are shown as the mean ± SD); (c) The whole-cell extract was prepared, and western blot analysis was performed with specific antibodies against indicated proteins. The immunoblots are representative of three independent experiments

Discussion

Advances in the treatment of BCP-ALL have dramatically improved survival rates. However, for relapsed patients or those who do not respond to conventional chemotherapy, the application of novel therapeutic modalities seems indispensable. Proteasome inhibition has been recently proposed as a promising targeting strategy for hematological malignancies (15). Numerous studies in different hematological and non-hematological malignancies have shown that PIs induce apoptosis in malignant cells (16, 17). Bortezomib is the first FDA-approved inhibitor for the treatment of patients with multiple myeloma and mantle cell lymphoma. It has already been documented that plasma proteasome activity was elevated in a large cohort of patients with ALL relative to healthy controls (18). Although a clinical trial with bortezomib in children with refractory/relapsed BCP-ALL yielded favorable results, serious side effects were challenging (19). Thus, second-generation PIs such as carfilzomib with less toxic side effects and minimal drug resistance was introduced. In the present study, we found that carfilzomib inhibits cell growth of BCP-ALL cells, which may be due to the induction of G2/M cell cycle arrest in addition to apoptotic cell death. Consistent with other studies (17, 20, 21), G2/M cell cycle arrest was observed in carfilzomib-treated BCP-ALL cell lines, and two key CDKIs, p21, and p27 were upregulated in the cells. As reported, UPS plays a crucial role in the regulation of p53 protein degradation (10), which is in line with our findings that carfilzomib effectively induced the accumulation of p53 protein levels in the BCP-ALL cells. Inactivation of the TP53 tumor suppressor gene via somatic mutations causes resistance to chemoradiation therapy that kills malignant cells via apoptotic signals. Since most pediatric BCP-ALLs bear wild-type p53, activating the p53 pathway by PIs represents a potentially effective treatment strategy (22). When DNA is damaged, p53 either repairs DNA or induces cell apoptosis. Moreover, p53 mediates G1 or G2/M arrest mainly through the upregulation of its target gene p21 (23, 24). Therefore, carfilzomib treatment can cause BCP-ALL cells to arrest in G2 by inhibiting p21 proteasomal degradation and increasing p53 accumulation. Furthermore, p27 is another cell cycle regulator that is degraded by the proteasome (25). We observed that carfilzomib-induced G2/M block in the BCP-ALL cells was accompanied by marked upregulation of p27. The results of our study corroborate previous studies indicating the PIs induced-G2/M arrest along with increased levels of p27 and p21 proteins (25, 26).

In line with several studies on solid tumors and hematological malignancies, the results of the present study showed that CFZ significantly induced dose- and time-dependent apoptosis and also potentiated

[DOI: 10.18502/ijpho.v13i2.12339]

sensitivity of BCP-ALL cells to the cytotoxic effects of doxorubicin and dexamethasone. Moreover, previous studies implicated the interplay between two independent regulatory mechanisms, caspase-mediated cleavage and proteasomal degradation of proteins, for fine-tuning cellular proteolysis. The proteasome can regulate apoptosis under its ability to degrade caspases and pro-apoptotic proteins. Conversely, induction of apoptosis results in caspase-mediated inactivation of the proteasome. Therefore, proteasome inhibition can shift the balance between these two regulatory mechanisms towards apoptosis by caspase-mediated degradation of survival proteins (27). Several pieces of evidence suggest that PIs mediate apoptosis through caspase activation and PARP cleavage in various cell lines (26, 28). The results of the present study showed that activation of caspases-3/9 and PARP cleavage increased incrementally upon escalating doses of carfilzomib in both BCP-ALL cell lines suggesting a caspase-dependent mechanism for carfilzomib cytotoxicity.

The c-Myc proto-oncogene is a transcriptional regulator of cell proliferation. Its cellular level is tightly regulated in several steps, including transcription, translation, and protein stability (29). Given its physiological degradation by the proteasome complex, some observations have suggested that PIs can upregulate c-Myc expression (30, 31). However, our data, in agreement with other studies, indicated that carfilzomib-induced cell death is strongly associated with c-Myc downregulation. One possible reason could be the negative regulatory role of elevated p53 on c-Myc expression (12). Furthermore, the p53 downstream target gene, p21, can cause c-Myc repression (32). Likewise, carfilzomib decreases the sumoylated Heterogeneous Nuclear Ribonucleoprotein K (hnRNP K), which upregulates c-Myc expression (33). BCP-ALL cells express high levels of Bcl-2 protein, which confers a survival advantage to lymphoblasts (34). A recent study by the Letai group has indicated Bcl-2 dependency of ALL cells, supporting the potential ability of Bcl-2 antagonists to improve current ALL therapies (35). Our findings revealed a significant decrease in Bcl-2 protein and mRNA levels upon exposure of BCP-ALL cell lines to carfilzomib. Mcl-1 is an anti-apoptotic protein that directly interacts with Bim and plays a major role in the regulation of apoptosis. In this context, the role of p53 and its target gene Noxa is unique because an increase in p53 or Noxa releases Bim from Mcl-1 and then activates the Bax/Bak complex through a "hit and run" mechanism (36, 37). We found that Noxa, Bim, and Bax expression increased significantly in carfilzomib-treated BCP-ALL cells, which could be one of the possible mechanisms of apoptosis upon proteasome inhibition by carfilzomib. Moreover, the Bax/Bcl-2 ratio was increased which drives the cells toward apoptosis.

The inhibitors of apoptosis proteins (IAPs) are a family of key regulators of apoptosis that bind to caspases and block their activity. Overexpression of IAPs and its association with chemoresistance have been indicated in many types of cancer (38). XIAP, the most potent member of the IAPs family, inhibits the intrinsic and extrinsic apoptosis pathways (39). In this study, we showed the depletion of c-IAP1 and XIAP proteins coupled with increased caspase activation after carfilzomib treatment in BCP-ALL cells. Survivin is another member of the IAPs family that plays a significant role in carcinogenesis (40). The role of survivin in PIs-induced apoptosis has not been fully understood. Some paradoxical reports were noted about the effect of bortezomib on survivin expression (41). Survivin is negatively regulated by wild-type p53. In p53-mutated or -null malignant cells, bortezomib upregulates survivin expression, whereas, in wild-type p53-expressing cancer cells, it declines or

[DOI: 10.18502/ijpho.v13i2.12339]

shows no significant effect on survivin expression (42, 43); Thus, in BCP-ALL cells harboring wild-type p53, a downregulatory effect of carfilzomib on survivin expression is expected.

Maintaining telomere length by the telomerase enzyme plays a vital role in carcinogenesis. hTERT is the critical component of the human telomerase complex controlling the activity of telomerase. In the majority of normal human somatic cells, hTERT expression is repressed, but overexpression and high levels of activity are found in most human cancer cells (44). Recent studies have shown that activation of wild-type p53 and overexpression of p21 can suppress hTERT expression (14, 45-47). Noteworthy, it seems that p53-mediated downregulation of hTERT is important for effective p53-dependent apoptosis (48). In addition, previous studies have indicated that the phosphorylation of c-Myc by survivin directly regulates the transcriptional expression of the hTERT gene (13). Thus, the most proper description of our findings is that p53-mediated downregulation of c-Myc and survivin, coupled with hTERT suppression, can reduce cell survival in carfilzomib-treated BCP-ALL cells.

Although carfilzomib alone has displayed significant effectiveness in clinical trials (49, 50), previous research has shown that proteasome inhibitors can lead to drug resistance (7). In addition, bortezomib has shown minimal effectiveness as a single agent in AML (51) and pediatric ALL (19). Nevertheless, numerous studies have demonstrated a synergistic combination of PIs with currently used anti-leukemic agents. For instance, bortezomib showed a synergistic effect with etoposide in multiple myeloma (52) and with cytarabine in AML and mantle cell lymphoma (53). Furthermore, bortezomib exhibited additive activity with cytarabine and vincristine in primary leukemic cells and cell lines (54). Some studies demonstrated that two basic drugs in the treatment of ALL, doxorubicin and dexamethasone, could activate or inactivate the proteasome system, respectively (55, 56). Intriguingly, our data showed that the treatment of BCP-ALL cells with carfilzomib and doxorubicin or dexamethasone synergistically reduces cell viability.

Conclusion

Taken together, our results suggested that carfilzomib had anti-tumor activity against BCP-ALL cells through p53-mediated p21 induction coupled with downregulation of c-Myc and hTERT transcription, which provides a promising therapeutic strategy for BCP-ALL patients, either as a single agent or in combination modality strategies. Despite this, clinical trials are required to evaluate the therapeutic potential of carfilzomib in the treatment of ALL.

Acknowledgments

The present paper is derived from a Ph.D. thesis supported by grant No. 28900 from the Iran University of Medical Sciences. The authors especially thank the deputy of Research & Technology of Iran University of Medical Sciences for supporting this study.

Conflict of interest

The authors declare no conflict of interest.

References

1. Hefazi M, Litzow MR. Recent advances in the biology and treatment of B-cell acute lymphoblastic leukemia. Blood Lymphat Cancer 2018;8:47-61.
2. Cooper SL, Brown PA. Treatment of pediatric acute lymphoblastic leukemia. Pediatr Clin North Am 2015;62(1):61-73.
3. Nooka A, Gleason C, Casbourne D, Lonial S. Relapsed and refractory lymphoid neoplasms and multiple myeloma with a focus on carfilzomib. Biologics 2013;7:13-32.

[DOI: 10.18502/ijpho.v13i2.12339]

4. Ma W, Kantarjian H, Zhang X, Wang X, Estrov Z, O'Brien S, et al. Ubiquitin-proteasome system profiling in acute leukemias and its clinical relevance. Leuk Res 2011;35(4):526-33.
5. Thomas X. Novel approaches to pediatric leukemia treatment. Expert Rev Anticancer Ther 2015;15(7):811-28.
6. Shen M, Schmitt S, Buac D, Dou QP. Targeting the ubiquitin-proteasome system for cancer therapy. Expert Opin Ther Targets 2013;17(9):1091-108.
7. Manasanch EE, Orlowski RZ. Proteasome inhibitors in cancer therapy. Nat Rev Clin Oncol 2017;14(7):417-33.
8. Burke MJ, Ziegler DS, Bautista Sirvent FJ, Attarbaschi A, Gore L, Locatelli F, et al. Phase 1b Study of Carfilzomib in Combination with Induction Chemotherapy in Children with Relapsed or Refractory Acute Lymphoblastic Leukemia (ALL). ASH Washington, DC; 2019.
9. Hientz K, Mohr A, Bhakta-Guha D, Efferth T. The role of p53 in cancer drug resistance and targeted chemotherapy. Oncotarget 2017;8(5):8921-46.
10. Tsvetkov P, Reuven N, Shaul Y. Ubiquitin-independent p53 proteasomal degradation. Cell Death Differ 2010;17(1):103-108.
11. Gupta SV, Hertlein E, Lu Y, Sass EJ, Lapalombella R, Chen TL, et al. The proteasome inhibitor carfilzomib functions independently of p53 to induce cytotoxicity and an atypical NF-kappaB response in chronic lymphocytic leukemia cells. Clin Cancer Res 2013;19(9):2406-2419.
12. Sachdeva M, Zhu S, Wu F, Wu H, Walia V, Kumar S, et al. p53 represses c-Myc through induction of the tumor suppressor miR-145. PNAS 2009;106(9):3207-3212.
13. Endoh T, Tsuji N, Asanuma K, Yagihashi A, Watanabe N. Survivin enhances telomerase activity via up-regulation of specificity protein 1- and c-Myc-mediated human telomerase reverse transcriptase gene transcription. Exp Cell Res 2005;305(2):300-311.
14. Beitzinger M, Oswald C, Beinoraviciute-Kellner R, Stiewe T. Regulation of telomerase activity by the p53 family member p73. Oncogene 2006;25(6):813-826.
15. Du XL, Chen Q. Recent advancements of bortezomib in acute lymphocytic leukemia treatment. Acta Haematol 2013;129(4):207-214.
16. Liu R, Fu C, Sun J, Wang X, Geng S, Wang X, et al. A New Perspective for Osteosarcoma Therapy: Proteasome Inhibition by MLN9708/2238 Successfully Induces Apoptosis and Cell Cycle Arrest and Attenuates the Invasion Ability of Osteosarcoma Cells in Vitro. Cell Physiol Biochem 2017;41(2):451-465.
17. Liu H, Westergard TD, Cashen A, Piwnica-Worms DR, Kunkle L, Vij R, et al. Proteasome inhibitors evoke latent tumor suppression programs in pro-B MLL leukemias through MLL-AF4. Cancer Cell 2014;25(4):530-542.
18. Krawczuk-Rybak M, Leszczynska E, Malinowska I, Matysiak M, Ostrowska H. Proteasome chymotrypsin-like activity in plasma as a useful marker for children with acute lymphoblastic leukemia. Scand J Clin Lab Invest 2012;72(1):67-72.
19. Messinger YH, Gaynon PS, Sposto R, van der Giessen J, Eckroth E, Malvar J, et al. Bortezomib with chemotherapy is highly active in advanced B-precursor acute lymphoblastic leukemia: Therapeutic Advances in Childhood Leukemia & Lymphoma (TACL) Study. Blood 2012;120(2):285-290.
20. Colado E, Alvarez-Fernandez S, Maiso P, Martin-Sanchez J, Vidriales MB, Garayoa M, et al. The effect of the proteasome inhibitor bortezomib on acute myeloid leukemia cells and drug resistance associated with the CD34+ immature phenotype. Haematologica 2008;93(1):57-66.
21. Gao M, Chen G, Wang H, Xie B, Hu L, Kong Y, et al. Therapeutic potential and functional interaction of carfilzomib

[DOI: 10.18502/ijpho.v13i2.12339]

and vorinostat in T-cell leukemia/lymphoma. Oncotarget 2016;7(20):29102-29115.
22. Kazemi A, Safa M, Shahbazi A. RITA enhances chemosensivity of pre-B ALL cells to doxorubicin by inducing p53-dependent apoptosis. Hematology 2011;16(4):225-231.
23. Davies C, Hogarth LA, Mackenzie KL, Hall AG, Lock RB. p21WAF1 modulates drug-induced apoptosis and cell cycle arrest in B-cell precursor acute lymphoblastic leukemia. Cell Cycle 2015;14(22):3602-3612.
24. Bunz F, Dutriaux A, Lengauer C, Waldman T, Zhou S, Brown JP, et al. Requirement for p53 and p21 to sustain G2 arrest after DNA damage. Science 1998;282(5393):1497-1501.
25. Zhou Y, Wang K, Zhen S, Wang R, Luo W. Carfilzomib induces G2/M cell cycle arrest in human endometrial cancer cells via upregulation of p21(Waf1/Cip1) and p27(Kip1). Taiwan J Obstet Gynecol 2016;55(6):847-851.
26. Augello G, Modica M, Azzolina A, Puleio R, Cassata G, Emma MR, et al. Preclinical evaluation of antitumor activity of the proteasome inhibitor MLN2238 (ixazomib) in hepatocellular carcinoma cells. Cell Death Dis 2018;9(2):28-35.
27. Gray DC, Mahrus S, Wells JA. Activation of specific apoptotic caspases with an engineered small-molecule-activated protease. Cell 2010;142(4):637-646.
28. Han B, Yao W, Oh YT, Tong JS, Li S, Deng J, et al. The novel proteasome inhibitor carfilzomib activates and enhances extrinsic apoptosis involving stabilization of death receptor 5. Oncotarget 2015;6(19):17532-17542.
29. Arabi A, Rustum C, Hallberg E, Wright AP. Accumulation of c-Myc and proteasomes at the nucleoli of cells containing elevated c-Myc protein levels. J Cell Sci 2003;116(Pt 9):1707-1717.
30. Li S, Jiang C, Pan J, Wang X, Jin J, Zhao L, et al. Regulation of c-Myc protein stability by proteasome activator REGgamma. Cell Death Differ 2015;22(6):1000-1011.
31. Edwards SK, Han Y, Liu Y, Kreider BZ, Liu Y, Grewal S, et al. Signaling mechanisms of bortezomib in TRAF3-deficient mouse B lymphoma and human multiple myeloma cells. Leuk Res 2016;41:85-95.
32. Vigneron A, Cherier J, Barré B, Gamelin E, Coqueret O. The cell cycle inhibitor p21waf1 binds to the myc and cdc25A promoters upon DNA damage and induces transcriptional repression. JBC 2006;281(46):34742-34750.
33. Suk FM, Lin SY, Lin RJ, Hsine YH, Liao YJ, Fang SU, et al. Bortezomib inhibits Burkitt's lymphoma cell proliferation by downregulating sumoylated hnRNP K and c-Myc expression. Oncotarget 2015;6(28):25988-26001.
34. Coustan-Smith E, Kitanaka A, Pui CH, McNinch L, Evans WE, Raimondi SC, et al. Clinical relevance of BCL-2 overexpression in childhood acute lymphoblastic leukemia. Blood 1996;87(3):1140-1146.
35. Moore VDG, Schlis KD, Sallan SE, Armstrong SA, Letai A. BCL-2 dependence and ABT-737 sensitivity in acute lymphoblastic leukemia. Blood 2008;111(4):2300-2309.
36. Gomez-Bougie P, Wuilleme-Toumi S, Menoret E, Trichet V, Robillard N, Philippe M, et al. Noxa up-regulation and Mcl-1 cleavage are associated to apoptosis induction by bortezomib in multiple myeloma. Cancer Res 2007;67(11):5418-5424.
37. Han J, Goldstein LA, Hou W, Gastman BR, Rabinowich H. Regulation of mitochondrial apoptotic events by p53-mediated disruption of complexes between antiapoptotic Bcl-2 members and Bim. J Biol Chem 2010;285(29):22473-22483.
38. Carter BZ, Mak DH, Wang Z, Ma W, Mak PY, Andreeff M, et al. XIAP downregulation promotes caspase-dependent inhibition of proteasome

[DOI: 10.18502/ijpho.v13i2.12339]

activity in AML cells. Leuk Res 2013;37(8):974-979.
39. Deveraux QL, Takahashi R, Salvesen GS, Reed JC. X-linked IAP is a direct inhibitor of cell-death proteases. Nature 1997;388(6639):300-304.
40. Li F, Ling X. Survivin Study: An update of "What is the next wave?. J. Cell. Physiol 2006;208(3):476-486.
41. Ling X, Calinski D, Chanan-Khan AA, Zhou M, Li F. Cancer cell sensitivity to bortezomib is associated with survivin expression and p53 status but not cancer cell types. J Exp Clin Cancer Res 2010;29:8-12.
42. Mirza A, McGuirk M, Hockenberry TN, Wu Q, Ashar H, Black S, et al. Human survivin is negatively regulated by wild-type p53 and participates in p53-dependent apoptotic pathway. Oncogene 2002;21(17):2613-2618.
43. Adamkov M, Halasova E, Rajcani J, Bencat M, Vybohova D, Rybarova S, et al. Relation between expression pattern of p53 and survivin in cutaneous basal cell carcinomas. Med. Sci. Monit 2011;17(3):BR74-79.
44. Amini A, Ghaffari SH, Mortazavi Y, Daliri K, Taranejoo S, Alimoghadam K, et al. Expression pattern of hTERT telomerase subunit gene in different stages of chronic myeloid leukemia. Mol Biol Rep 2014;41(9):5557-5561.
45. Kusumoto M, Ogawa T, Mizumoto K, Ueno H, Niiyama H, Sato N, et al. Adenovirus-mediated p53 gene transduction inhibits telomerase activity independent of its effects on cell cycle arrest and apoptosis in human pancreatic cancer cells. Clin Cancer Res 1999;5(8):2140-2147.
46. Wang Z, Kyo S, Takakura M, Tanaka M, Yatabe N, Maida Y, et al. Progesterone regulates human telomerase reverse transcriptase gene expression via activation of mitogen-activated protein kinase signaling pathway. Cancer Res 2000;60(19):5376-5381.
47. Safa M, Tavasoli B, Manafi R, Kiani F, Kashiri M, Ebrahimi S, et al. Indole-3-carbinol suppresses NF-kappaB activity and stimulates the p53 pathway in pre-B acute lymphoblastic leukemia cells. Tumour Biol 2015;36(5):3919-3930.
48. Rahman R, Latonen L, Wiman KG. hTERT antagonizes p53-induced apoptosis independently of telomerase activity. Oncogene 2005;24(8):1320-1327.
49. Jakubowiak AJ, Siegel DS, Martin T, Wang M, Vij R, Lonial S, et al. Treatment outcomes in patients with relapsed and refractory multiple myeloma and high-risk cytogenetics receiving single-agent carfilzomib in the PX-171-003-A1 study. Leukemia 2013;27(12):2351-2356.
50. O'Connor OA, Stewart AK, Vallone M, Molineaux CJ, Kunkel LA, Gerecitano JF, et al. A phase 1 dose escalation study of the safety and pharmacokinetics of the novel proteasome inhibitor carfilzomib (PR-171) in patients with hematologic malignancies. Clin Cancer Res 2009;15(22):7085-7091.
51. Cortes J, Thomas D, Koller C, Giles F, Estey E, Faderl S, et al. Phase I study of bortezomib in refractory or relapsed acute leukemias. Clin Cancer Res 2004;10(10):3371-3376.
52. von Metzler I, Heider U, Mieth M, Lamottke B, Kaiser M, Jakob C, et al. Synergistic interaction of proteasome and topoisomerase II inhibition in multiple myeloma. Exp Cell Res 2009;315(14):2471-2478.
53. Weigert O, Pastore A, Rieken M, Lang N, Hiddemann W, Dreyling M. Sequence-dependent synergy of the proteasome inhibitor bortezomib and cytarabine in mantle cell lymphoma. Leukemia 2007;21(3):524-528.
54. Horton TM, Gannavarapu A, Blaney SM, D'Argenio DZ, Plon SE, Berg SL. Bortezomib interactions with chemotherapy agents in acute leukemia in vitro. Cancer Chemother Pharmacol 2006;58(1):13-23.

[DOI: 10.18502/ijpho.v13i2.12339]

55. Ortiz-Lazareno PC, Bravo-Cuellar A, Lerma-Díaz JM, Jave-Suárez LF, Aguilar-Lemarroy A, Domínguez-Rodríguez JR, et al. Sensitization of U937 leukemia cells to doxorubicin by the MG132 proteasome inhibitor induces an increase in apoptosis by suppressing NF-kappa B and mitochondrial membrane potential loss. Cancer cell international 2014;14(1):13-18.
56. Beyette J, Mason GG, Murray RZ, Cohen GM, Rivett AJ. Proteasome activities decrease during dexamethasone-induced apoptosis of thymocytes. Biochem J 1998;332 (Pt 2)(2):315-320.

[DOI: 10.18502/ijpho.v13i2.12339]